RJC

RASĀYAN *J. Chem.*
Vol. 15 | No. 4 |2969-2975| October - December | 2022
ISSN: 0974-1496 | e-ISSN: 0976-0083 | CODEN: RJCABP
http://www.rasayanjournal.com
http://www.rasayanjournal.co.in

EFFECT OF METAL CONCENTRATION ON PHYSICOCHEMICAL PROPERTIES OF COBALT/REDUCED GRAPHENE OXIDE THROUGH ONE-POT GREENER CHEMICAL-THERMAL REDUCTION USING ULTRASONIC ACTIVATION

Dyah Ayu Fatmawati, Triyono✉, Wega Trisunaryanti, and Uswatul Chasanah
Department of Chemistry, Faculty of Mathematics and Natural Sciences,
Universitas Gadjah Mada, D.I. Yogyakarta, 55281, Indonesia
✉Corresponding Author: triyn102@ugm.ac.id

ABSTRACT

A combination of ultrasonically supported one-step chemical thermal reductions for synthesizing cobalt/reduced graphene oxide (Co/RGO) has been successfully carried out. This study aims to investigate the variation of Co concentration to GO (1, 5, and 10% w/w) on its physicochemical properties. GO precursor was prepared by the Tour method with an oxidizing agent:graphite weight ratio of 3.5. According to the findings of the investigation, in XRD spectra, the reduction treatment succeeded in shifting the diffraction peaks from 10° of GO to ~24° of Co/RGO. In FTIR spectra, the intensity of absorption peaks of O-H and C=O vibrations decreased after reduction. In SAA isotherm, Co-5/RGO material has the largest specific surface area of 109.753 m^2/g with a pore volume of 0.158 cc/g and a pore diameter of 3.469 nm. Thus, this ratio (5% w/w) is the most optimal Co concentration that can be loaded to GO material.

Keywords: Cobalt, Co-reduction, Reduced Graphene Oxide, Sonochemical, Tour Method

RASĀYAN *J. Chem.*, Vol. 15, No.4, 2022

INTRODUCTION

Graphene is a crystal that exists in two dimensions (2D) with a basal monatomic layer of hexagonally packed sp^2-conjugated carbon atoms. It was predicted theoretically a long time ago but was not manufactured until 2004.[1] As a new material, the use of graphene is very attractive. This is due to the many interesting mechanical, thermal, and electrical properties reported that confirm the superiority of graphene over traditional materials.[2] Graphene can be produced in a variety of ways, including chemical vapor deposition, mechanical exfoliation, cleavage and annealing of single crystal SiC under ultra-high vacuum.[3] However, due to the high cost and low capacity of current manufacturing methods, commercial applications of graphene remains limited.[4] In general, mass production of individual graphene foils has proven to be a major challenge. This issue can be resolved through the chemical reduction of graphene oxide (GO) (hydrazine, dimethylhydrazine, hydroquinone, sodium borohydride, etc.).[5] However, reducing chemicals are either harmful to the environment, toxic, or both. As a result, new approaches were needed to effectively convert GO to reduced graphene oxide (RGO) under mild conditions. With its mild reducing power and non-toxic properties, L-ascorbic acid (LAA) is naturally used as a reducing agent for living organisms and has also been used as the main reducing agent when GO is converted to RGO.[6] Based on the literature, as a powerful reducing agent, L-ascorbic acid performs two functions in this process: hydrophilic GO is reduced to hydrophobic RGO, and the remaining Mn (VII) ions are converted to soluble Mn (II) ions.[4] RGO is excellent support for nanocomposites because it has a large specific surface area and can evenly disperse nanoparticles (NPs). In addition, structural defects in RGO can contribute to the higher dispersion of NPs composites.[7] As a result of its extensive specific surface area, excellent biocompatibility, and high adsorption capacity for specific molecules, graphene, and its derivatives can be used as a valuable substrate for interaction with various species, as a catalytic carrier, or as the only catalyst.[8] The functionalization of GO by metal NPs can improve the characteristics of electrochemical sensors by the additional electro-catalytic function.[9] The formation of graphene-NP composites has opened new and diverse paths for

http://doi.org/10.31788/RJC.2022.1546923

research and application. Inexpensive and widely used transition metals can be a good alternative to precious metals in electrochemical sensor applications.[10] Because of its high theoretical specific capacitance of 3580 F g^{-1}, excellent electrochemical redox activity, and excellent reversibility, Co_3O_4 is a promising candidate for these applications.[11] The composite can have different magnetic properties than the individual components shown in the graphene-Co_3O_4 composite, the composite is superparamagnetic and pure Co_3O_4 is antiferromagnetic.[12] Researchers have used cobalt, one of the essential 3d metals readily available, in large-scale catalytic processes. Co nanocomposites are also excellent candidates for ferrofluids, drug delivery, hyperthermia, and magnetic imaging applications.[13] In addition, mechanical treatment in some parts to obtain graphene was thought to contribute to the collapse of the Van der Waals forces between the graphite layers due to the high potential. Sonication of graphite in the oxidant may strip the oxidized layer and expose the inner layer to the chemical oxidant.[14] Sonochemical synthesis of metals, metal oxides, and metal sulfides has proven to be an adaptable and promising technique in recent years.[15] The chemical effect of ultrasonic radiation results from the phenomenon of acoustic cavitation. When ultrasonic waves are used to irradiate a liquid, bubbles are generated, and when the bubbles grow and collapse, ultrasonic energy is accumulated and the stored energy is quickly released. These cavitation implosions create local hotspots at high temperatures of 5000 K, pressures of 1000 bar, and heating and cooling rates of 1010 K/s.[16] According to the literature, sonochemistry is a unique chemical method for producing nanomaterials without high pressure, high temperature, or long reaction times.[17] Several researchers study about CoNPs deposited on RGO with ultrasonic wave-assisted reduction heating such as Akhtar *et al.* (2013)[18] and Gao *et al.* (2019).[19] However, these researchers used GO precursors synthesized through the Hummers method. Recent research was conducted by Torshizi *et al.* (2021)[20] with the same research model, but they also evaluated the loading weight of Co on RGO. The Hummers method has received the most attention because of its efficiency and high level of responsiveness, but it still has two drawbacks. First, the oxidation process releases toxic gas, and second, the remaining sodium and nitrate ions in the wastewater from the GO synthesis and purification process are difficult to remove.[21] Tour *et al*. can improve the Hummers method by eliminating the use of $NaNO_3$, increasing the amount of $KMnO_4$, and introducing a new medium into the reaction system via a mixture of H_2SO_4/H_3PO_4 acids (9/1 v/v).[22] This modification has proven to be successful in increasing the reaction yield, preventing the formation of holes, and also reducing the emission of toxic gases. So far, the recommended ratio of graphite:$KMnO_4$ is 1:6 with a synthesis time of 24 hours.[23] However, in this study, a ratio of 1:3.5[24] was used with a synthesis time of 6 hours.[25] This method is now more efficient and adheres to green chemistry principles. Therefore, in this study, we synthesized CoNPs with various concentrations dispersed onto the surface of RGO using GO precursors from weight ratio graphite:$KMnO_4$ of 1:3.5 prepared by the Tour method. This working procedure is carried out by one step of ultrasonic treatment-assisted chemical reduction. All physicochemical properties of the Co/RGO material will be studied further through the characterization results of the XRD, FTIR, SAA, SEM-EDX, and TEM.

EXPERIMENTAL

Materials

All materials applied in this experiment were from commercial sources (E-Merck Germany) with analytical grade (p.a) and were implemented without subsequent purification. Materials used involved graphite powder, potassium permanganate, sulfuric acid 98%, ortho-phosphoric acid 85%, hydrogen peroxide 30%, hydrochloric acid 37%, absolute ethanol, cobalt (II) nitrate hexahydrate, sodium hydroxide, L(+)-ascorbic acid, silver nitrate, and barium chloride. For washing the materials, deionized (DI) water, phosphate-buffered saline (PBS), and bi-distilled water were utilized.

Synthesis of Graphene Oxide (GO)

A mixture of 0.375 g graphite and 1.3125 g potassium permanganate (weight ratio of 1:3.5) was reacted in a mixture of 45 mL sulfuric acid and 5 mL phosphoric acid (9:1 volume ratio) for 6 h at a temperature of 65 °C under stirring. Previously, each mixture was cooled in a refrigerator for 1 h to avoid an exothermic oxidation reaction. After the reaction has been completed, the solution is allowed to reach room temperature, then poured into a beaker containing 200 mL DI ice, followed by the addition of 3 mL hydrogen peroxide to stop the oxidation reaction. The resulting material was washed with hydrochloric acid, ethanol, PBS, and bi-distilled water, successively until it reached a neutral pH and was free of sulfate

and chloride ions (checked using barium chloride and silver nitrate). Finally, the material obtained was dried in an oven at 80 °C for 12 h.

Synthesis of Cobalt/reduced Graphene Oxide (Co/RGO)

Synthesis of Co nanoparticles (CoNPs) decorated onto the RGO surface was carried out by a one-pot chemical-thermal reduction method. First, the cobalt (II) nitrate hexahydrate solution as a salt precursor (with variations in the amount of Co concentration to GO of 1.0, 5.0, and 10% w/w) was stirred for 10 min at room temperature followed by the addition of GO dispersion. The reaction mixture was stirred for 10 min and then 0.1 M NaOH solution was added to raise the pH of the mixture to 9. The reaction mixture was stirred for 5 min followed by the addition of L-ascorbic acid solution as a reducing agent (weight ratio of ascorbic acid to GO of 10). Stirring was continued for 10 min then followed by ultrasonic waves-assisted heating using a sonicator instrument for 30 min at 70 °C. The reaction mixture then changes color to a black solution which indicates the formation of nanostructures. The obtained Co/RGO nanostructures were washed several times using bi-distilled water through centrifugation and then dried in an oven at 60 °C for 12 h.

Detection Method

X-Ray Diffraction (XRD, Philips X'Pert MPD) at a wide angle of 5–90° was used to determine the crystallinity of the materials. The functional groups of the materials were characterized by Fourier Transform Infra-Red Spectrometer (FTIR, Shimadzu Prestige 21) at 4000–400 cm^{-1}. The Surface Area Analyzer (SAA, JWGB Meso 112) was used to analyze the textural properties of materials such as specific surface area, pore volume, and pore diameter which are calculated using the BET and BJH approaches. The image of the material's nanostructure was taken using a Transmission Electron Microscope (TEM, JEOL JEM-1400). The surface morphology and metal content of the materials were evaluated by Scanning Electron Microscope-Energy Dispersive X-ray (SEM-EDX, JSM-6510LA).

RESULTS AND DISCUSSION

It is known that the diffraction peak of pure graphite is at 2θ around 26º due to the interlayer distance of 3.4 Å.[26] In Fig.-1 (left side), the GO XRD pattern obtained by the improved Hummer (Tour) method reveals a sharp main diffraction peak at 2θ = 10.36° with the Miller index (002) planes that indicates the crystallinity of the material. This diffraction peak, with an inter-planar distance of 8.53 Å, is sufficient to characterize GO.[27] The disappearance of the peak at 26º proves that the resulting compound is completely oxidized by the post-treatment of graphite oxidation and exfoliation to form oxygenated functional groups.[28] After chemical-thermal reduction, a broader peak can be observed for Co-1/RGO, Co-5/RGO, Co-10/RGO at 2θ = 24.54, 23.06, 23.29º resulting in the d-spacing of 3.63, 3.85, 3.82 Å, respectively, demonstrating that oxygen-containing functional groups were effectively removed.[29] This leads to a defect in the crystal rearrangement of the π-conjugated graphene structure so that the diffraction peaks look amorphous. Another low-intensity peak is seen at about 42° in the (100) direction. It is assigned to the turbostratic band of chaotic carbon material.[30] It should be noted that during the synthesis process, Co^{2+} in the mixed solution was also reduced to metallic Co by L-ascorbic acid. However, no apparent diffraction peaks are observed for the XRD pattern of all Co/RGO composites. This indicates that the metal Co is in an amorphous state within the composite.[31] In addition, leaching may occur during the material washing process so that the remaining amount of Co is less than the instrument detection limit. As explained in the XRD discussion that these materials consist mostly of sp^2-hybridized carbon and a small portion of oxygen functional groups attached to both the graphene's basal and its edges.[32] Therefore, EDX analysis is needed to determine the percentage content of the main elements of these materials. The results of the analysis in Fig.-1 (right side) show the %mass C increasing and %mass O decreasing from GO to Co/RGO. This indicates that the chemical-ultrasonic reduction process was successful. The reduction level is represented by the magnitude of the C/O ratio. The value of the C/O ratio for GO, Co-1/RGO, Co-5/RGO, and Co-10/RGO is 1.46, 3.36, 3.24, and 4.35, successively. The decrease in the percentage of oxygen elements (about 40-50% of the initial oxygen content) strengthens the reason for the decrease in the distance between layers[33] and the emergence of amorphous properties of sp^3-type carbon defects. Meanwhile, the actual %mass of Co was lower than that loaded in the method due to leaching during material washing. This result reinforces the XRD data which

does not show any Co diffraction peaks due to its presence below the detection limit. The presence of Na, S, and K contents in GO indicates that the washing is not optimal so the residues of PBS, sulfuric acid, and potassium permanganate are still attached.

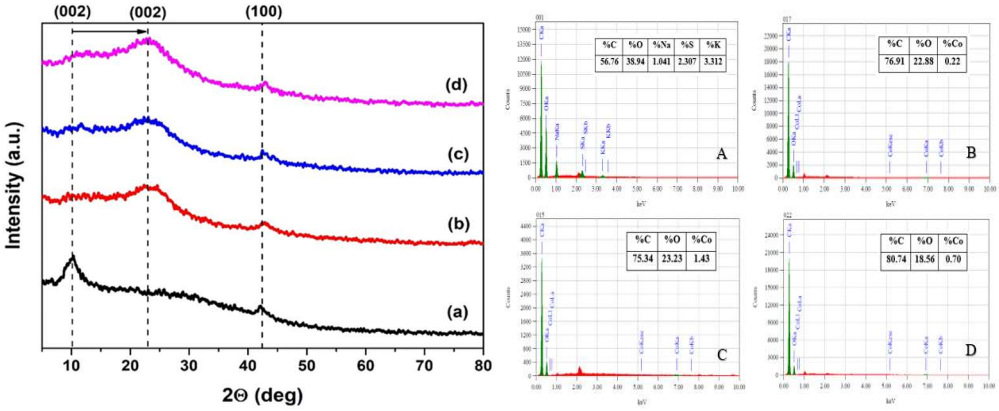

Fig.-1: XRD diffractograms (left side) and EDX spectra (right side) of (a) GO, (b) Co-1/RGO, (c) Co-5/RGO, and (d) Co-10/RGO

FTIR spectra in Fig.-2 were applied to confirm the types of oxygen-containing functional groups that caused the increase and decrease of d-spacing in the previous XRD data. The absorptions of functional groups recorded in the spectra include OH vibrations at 3448.72 cm^{-1}, C-H_{sp3} vibrations at 2931.80 cm^{-1}, CO_2 vibrations at 2337.72 cm^{-1}, C=O vibrations at 1600-1700 cm^{-1}, and C-O vibrations at 1000-1200 cm^{-1}. The existence of C=C vibration at 1527.62 cm^{-1} is because most of these materials consist of graphitic carbon.[34] All materials have a character that is not much different. However, after the reduction process of GO to Co/RGO, it decreased the absorption intensity of O-H and C=O.[35] The trend of decreasing intensity from GO to Co/RGO is supported by the C/O ratio value from EDX which describes the level of reduction. The order of reduction levels from lowest to highest is Co-5/RGO, Co-1/RGO, and Co-10/RGO.

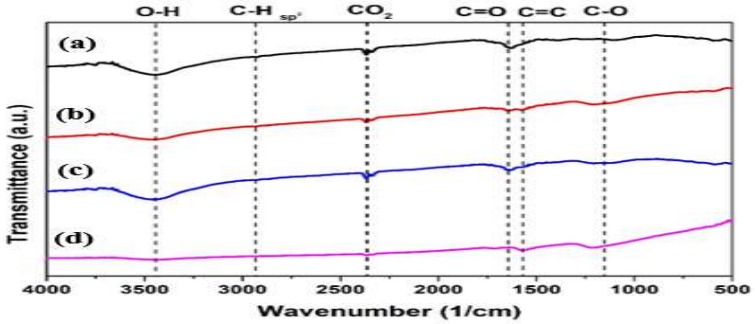

Fig.-2: FTIR Spectra of (a) GO, (b) Co-1/RGO, (c) Co-5/RGO, and (d) Co-10/RGO

The nitrogen adsorption-desorption isotherms (Fig.-3 (left side)) for these materials can be classified as representing Type V isotherms. Type V is usually owned by mesoporous materials where the isotherm is followed by the formation of a hysteresis loop which is associated with capillary condensation. All materials have H3-type hysteresis loops ranging from 0.5 to 1.0 P/P_0. This demonstrates the presence of micro-and mesoporous structures within the material layers with plate-like slit-shaped pores[36] or points out the formation of plate-like particle aggregates that form slit-like pores.[37] A comparatively large hysteresis loop of GO, Co-1/RGO, and Co-5/RGO in this relative pressure (P/P_0) range are a feature of an inhomogeneous hierarchically porous structure. However, the Co-10/RGO has a rather narrow and small hysteresis loop character. Here, the nitrogen adsorption volume decreases significantly which affects the specific surface area. This decrease may be related to the clogging of the openings between the layers due to the presence of metal groups.[38] The Barrett, Joyner, and Halenda (BJH) curve (Fig.-3 (right side)) indicates the presence of mesopore of diameter around 3 nm including 3.566 of GO, 3.321 of Co-1/RGO, 3.469 of Co-5/RGO, and 3.459 of Co-10/RGO.[39]

All of these materials are mesoporous because of not only the presence of a hysteresis loop in the above isotherm curves but also the pore diameter is in the range between 2-50 nm following the IUPAC rule.[40] Meanwhile, the pore volume of materials (cc/g) obtained is 0.319 of GO, 0.152 of Co-1/RGO, 0.158 of Co-5/RGO, and 0.087 of Co-10/RGO.

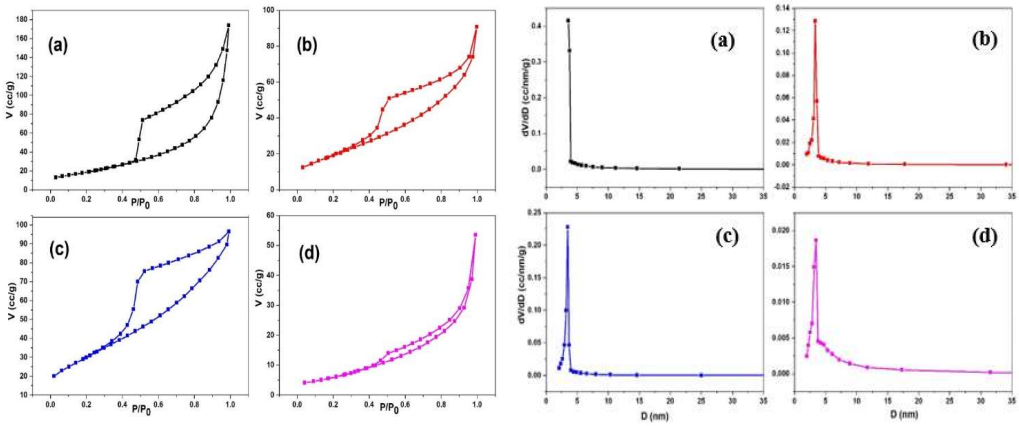

Fig.-3: N_2 isotherm pattern (left side) and Pore distribution (right side) of (a) GO, (b) Co-1/RGO, (c) Co-5/RGO, and (d) Co-10/RGO

The Brunauer, Emmett, and Teller (BET) surface area (m^2/g) of each material measured from the adsorption branch of the isotherm at low relative pressures is 69.331 of GO, 73.266 of Co-1/RGO, 109.753 of Co-5/RGO, and 24.086 of Co-10/RGO. From these data, it can be seen that there was an increase in the specific surface area after Co metal was deposited on the GO surface. This is because Co is evenly distributed to the surface of the supporting material. If viewed in more detail, there has been a drastic decrease in the surface area of Co-10/RGO, whereas the percentage of Co metal in Co-10/RGO is greater than Co-1/RGO according to previous EDX data. It is possible that the CoNPs formed on Co-10/RGO block the pores of the RGO material or agglomerate in some areas.[41] According to the findings of the analysis, it can be resumed that Co-5/RGO has the largest surface area among the others. Therefore, this concentration is most optimal in the Co/RGO synthesis for use as a catalyst/support material in various applications.

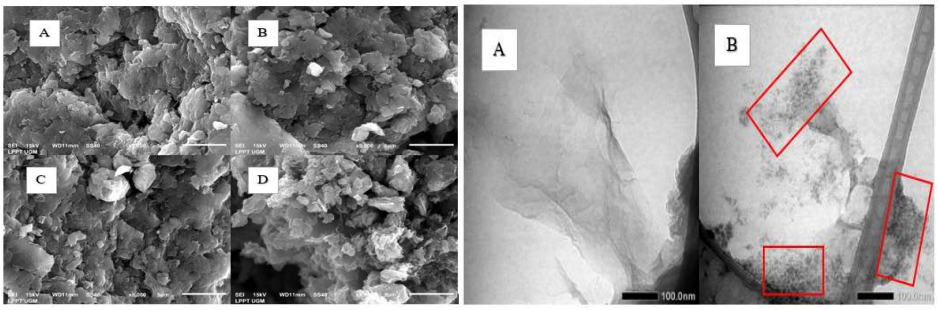

Fig.-4: SEM Micrograph (left side) of (a) GO, (b) Co-1/RGO, (c) Co-5/RGO, and (d) Co-10/RGO and TEM Images (right side) of (a) GO, (b) Co-10/RGO

The surface morphology of the material was imaged by SEM with the results displayed in Fig.-4 (left side). Both GO and Co/RGO materials appear as similar thin sheets randomly aggregated and exfoliated sheet-like material surface, with irregular, rough, distinct edges, wrinkled surfaces, and folding.[42] TEM images have both dark and light areas. The dark areas are stacked layers, while the bright areas are exfoliated layers. GO (Fig.-4 (right side, a)) looks almost transparent because it contains a higher concentration of oxygen-functionalized carbon that are suitable for exfoliation or intercalation.[24] After reduction treatment, Fig.-4 (right side, b) also shows the nanoscopic features of RGO–CoNPs with its layered structure.[43]

CONCLUSION

A one-step reduction method with a chemical-thermal combination of ultrasonic waves was used to successfully synthesize Cobalt/reduced graphene oxide (Co/RGO). The results obtained are that the

intensity of the absorption of FTIR vibrations on several oxygen functional groups is directly proportional to the level of reduction represented by the C/O ratio from the EDX data. In addition, the value of the specific surface area of the material also shows a relationship with the actual amount of metal deposited on the surface of the RGO. Based on the SAA analysis, Co-5/RGO material has the largest specific surface area among other materials due to the optimal amount of metal. Therefore, this material can be used as a catalyst in several future applications.

ACKNOWLEDGEMENT

The authors thank Universitas Gadjah Mada for the financial support of this work under the scheme of the *Rekognisi Tugas Akhir* (RTA) 2021 with assignment letter number: 3143/UN1.P.III/DIT-LIT/PT/2021 for Triyono.

REFERENCES

1. R. Tarcan, O. Todor-Boer, I. Petrovai, C. Leordean, S. Astilean, and I. Botiz, *Journal of Materials Chemistry C*, **8**, 1198(2020), https://doi.org/10.1039/c9tc04916a
2. S. Pei and H. M. Cheng, *Carbon*, **50**, 3210(2012), https://doi.org/10.1016/j.carbon.2011.11.010
3. V. Loryuenyong, K. Totepvimarn, P. Eimburanapravat, W. Boonchompoo, and A. Buasri, *Advances in Materials Science and Engineering*, **2013**, 923403(2013), https://doi.org/10.1155/2013/923403
4. S. Abdolhosseinzadeh, H. Asgharzadeh, and H. S. Kim, *Scientific Reports*, **5**, 10160(2015), https://doi.org/10.1038/srep10160
5. S. Sadhukhan, T. K. Ghosh, D. Rana, I. Roy, A. Bhattacharyya, G. Sarkar, M. Chakraborty, and D. Chattopadhyay, *Materials Research Bulletin*, **79**, 41(2016), https://doi.org/10.1016/j.materresbull.2016.02.039
6. A. T. Habte and D. W. Ayele, *Advances in Materials Science and Engineering*, **2019**, 5058163(2019), https://doi.org/10.1155/2019/5058163
7. J. R. Do Nascimento, M. R. D'oliveira, A. G. Veiga, C. A. Chagas, and M. Schmal, *ACS Omega*, **5**, 25568(2020), https://doi.org/10.1021/acsomega.0c02417
8. M. Hu, Z. Yao, and X. Wang, *Industrial and Engineering Chemistry Research*, **56**, 3477(2017), https://doi.org/10.1021/acs.iecr.6b05048
9. Z. Yang, C. Qi, X. Zheng, and J. Zheng, *New Journal of Chemistry*, **39**, 9358(2015), https://doi.org/10.1039/c5nj01621e
10. N. Sebastian, W. C. Yu, Y. C. Hu, D. Balram, and Y. H. Yu, *Ultrasonics Sonochemistry*, **59**, 104696(2019), https://doi.org/10.1016/j.ultsonch.2019.104696
11. T. T. Nguyen, V. H. Nguyen, R. K. Deivasigamani, D. Kharismadewi, Y. Iwai, and J. J. Shim, *Solid State Sciences*, **53**, 71(2016), https://doi.org/10.1016/j.solidstatesciences.2016.01.006
12. N. N. Malinga and A. L. L. Jarvis, *Journal of Nanostructure in Chemistry*, **10**, 55(2020), https://doi.org/10.1007/s40097-019-00328-7
13. N. Singh, J. R. Ansari, M. Pal, N. T. K. Thanh, T. Le, and A. Datta, *Journal of Materials Science: Materials in Electronics*, **31**, 15108(2020), https://doi.org/10.1007/s10854-020-04075-2
14. M. F. Zainuddin, N. H. Nik Raikhan, N. H. Othman, and W. F. H. Abdullah, *IOP Conference Series: Materials Science and Engineering*, **358**, 012046(2018), https://doi.org/10.1088/1757-899X/358/1/012046
15. A. M. Golsheikh, N. M. Huang, H. N. Lim, and R. Zakaria, *RSC Advances*, **4**, 36401(2014), https://doi.org/10.1039/c4ra05998k
16. A. M. Golsheikh, H. N. Lim, R. Zakaria, and N. M. Huang, *RSC Advances*, **5**, 12726(2015), https://doi.org/10.1039/c4ra14775h
17. N. Karikalan, R. Karthik, S. M. Chen, C. Karuppiah, and A. Elangovan, *Scientific Reports*, **7**, 2494(2017), https://doi.org/10.1038/s41598-017-02479-5
18. A. J. Akhtar, A. Gupta, B. Kumar Shaw, and S. K. Saha, *Applied Physics Letters*, **103**, 242902(2013), https://doi.org/10.1063/1.4845536
19. L. Gao, W. Zhuge, X. Feng, W. Sun, X. Sun, and G. Zheng, *New Journal of Chemistry*, **43**, 8189(2019), https://doi.org/10.1039/c9nj00470j
20. H. O. Torshizi, A. Nakhaei Pour, A. Mohammadi, Y. Zamani, and S. M. Kamali Shahri, *Frontiers of Chemical Science and Engineering*, **15**, 299(2021), https://doi.org/10.1007/s11705-020-1925-x

21. J. Chen, B. Yao, C. Li, and G. Shi, *Carbon*, **64**, 225(2013), https://doi.org/10.1016/j.carbon.2013.07.055
22. D. C. Marcano, D. V. Kosynkin, J. M. Berlin, A. Sinitskii, Z. Sun, A. Slesarev, L. B. Alemany, W. Lu, and J. M. Tour, *ACS Nano*, **4**, 4806(2010), https://doi.org/10.1021/nn1006368
23. P. Ranjan, S. Agrawal, A. Sinha, T. R. Rao, J. Balakrishnan, and A. D. Thakur, *Scientific Reports*, **8**, 12007(2018), https://doi.org/10.1038/s41598-018-30613-4
24. D. A. Fatmawati, T. Triyono, W. Trisunaryanti, H. S. Oktaviano, and U. Chasanah, *Rasayan Journal of Chemistry*, **14**, 2129(2021), https://doi.org/10.31788/RJC.2021.1436004
25. U. Chasanah, W. Trisunaryanti, Triyono, H. S. Oktaviano, and D. A. Fatmawati, *Rasayan Journal of Chemistry*, **14**, 2017(2021), https://doi.org/10.31788/RJC.2021.1436042
26. D. A. Fatmawati, T. Triyono, W. Trisunaryanti, H. S. Oktaviano, and U. Chasanah, *Indonesian Journal of Chemistry*, **21**, 1086(2021), https://doi.org/10.22146/ijc.57423
27. J. Lucas and M. Poulain, *Comptes Rendus Chimie*, **5**, 813(2002), https://doi.org/10.1016/S1631-0748(03)01461-9
28. M. Handayani, E. Sulistiyono, F. Rokhmanto, N. Darsono, P. L. Fransisca, A. Erryani, and J. T. Wardono, *IOP Conference Series: Materials Science and Engineering*, **578**, 012073(2019), https://doi.org/10.1088/1757-899X/578/1/012073
29. J. Zhang, A. Feng, J. Bai, Z. Tan, W. Shao, Y. Yang, W. Hong, and X. Zongyuan, *Nanoscale Research Letters*, **12**, 521(2017), https://doi.org/10.1186/s11671-017-2290-7
30. N. M. S. Hidayah, W. W. Liu, C. W. Lai, N. Z. Noriman, C. S. Khe, U. Hashim, and H. C. Lee, *AIP Conference Proceedings*, **1892**, 150002(2017), https://doi.org/10.1063/1.5005764
31. F. Paquin, J. Rivnay, A. Salleo, N. Stingelin, and C. Silva, *Journal of Materials Chemistry C*, **3**, 10715(2015), https://doi.org/10.1039/b000000x
32. D. Chen, H. Feng, and J. Li, *Chemical Reviews*, **112**, 6027(2012), https://doi.org/10.1021/cr300115g
33. M. Khan, A. H. Al-Marri, M. Khan, N. Mohri, S. F. Adil, A. Al-Warthan, M. R. H. Siddiqui, H. Z. Alkhathlan, R. Berger, W. Tremel, and M. N. Tahir, *RSC Advances*, **4**, 24119(2014), https://doi.org/10.1039/c4ra01296h
34. Sudesh, N. Kumar, S. Das, C. Bernhard, and G. D. Varma, *Superconductor Science and Technology*, **26**, 095008(2013), https://doi.org/10.1088/0953-2048/26/9/095008
35. X. Liu, X. Y. Shao, G. B. Fang, H. F. He, and Z. G. Wan, *E-Polymers*, **17**, 3(2017), https://doi.org/10.1515/epoly-2016-0094
36. N. P. D. Ngidi, M. A. Ollengo, and V. O. Nyamori, *Materials*, **12**, 3376(2019), https://doi.org/10.3390/ma12203376
37. P. P. A. Jose, M. S. Kala, A. V. Joseph, N. Kalarikkal, and S. Thomas, *Applied Physics A: Materials Science and Processing*, **26**, 58(2020), https://doi.org/10.1007/s00339-019-3237-x
38. S. B. Singh and M. De, *Journal of Materials Research*, **36**, 3109(2021), https://doi.org/10.1557/s43578-021-00331-1
39. C. Selvaraj, S. Kumar, N. Munichandraiah, and L. G. Scanlon, *Journal of The Electrochemical Society*, **161**, A554(2014), https://doi.org/10.1149/2.055404jes
40. R. J. White, V. Budarin, R. Luque, J. H. Clark, and D. J. Macquarrie, *Chemical Society Reviews*, **38**, 3401(2009), https://doi.org/10.1039/b822668g
41. M. L. Permata, W. Trisunaryanti, I. I. Falah, M. T. Hapsari, and D. A. Fatmawati, *Rasayan Journal of Chemistry*, **13**, 772(2020), https://doi.org/10.31788/RJC.2020.1315529
42. A. Shalaby, D. Nihtianova, P. Markov, A. D. Staneva, R. S. Iordanova, and Y. B. Dimitriev, *Bulgarian Chemical Communications*, **47**, 291(2015)
43. P. Kumar, A. Kumar, B. Sreedhar, B. Sain, S. S. Ray, and S. L. Jain, *Chemistry - A European Journal*, 20, 6154(2014), https://doi.org/10.1002/chem.201304189

[RJC-6923/2020]